



Karaj branch

Journal of  
Applied  
Chemical  
Research

jacr.kiau.ac.ir

*Journal of Applied Chemical Research, 11, 4, 60-73 (2017)*

## **Binuclear Complex of Zinc and Copper with Unsymmetrical Macrocyclic Ligand as Sensitizer in Nanocrystalline TiO<sub>2</sub> Solar Cells**

**Malihe Khalili, Mohammad Abedi\*, Davood Sadeghi Fateh, Kobra Razmi**

*Department of Chemical Technologies, Iranian Research Organization for Science and Technology (IROST), Tehran, Iran*

*(Received 12 Mar. 2017; Final version received 14 Jun. 2017)*

---

### **Abstract**

Dye sensitized solar cells (DSSCs) are considered as one of the most promising alternative renewable energy sources. In the structure of DSSCs, a photosensitizer composed of transition metal complexes is used to harvest light. In this work a binuclear complex containing two propionitrile pendant arms [ZnLCu(OAC)]PF<sub>6</sub> {L = 1, 6- bis (2-cyanoethyl) -2, 5-bis (2-hydroxy 3-formyl-5-methylbenzyl)-2, 5- diazahexane} has been examined as a non-planar metal based photosensitizer in the fabrication of dye sensitized solar cell. The photovoltaic performance of the fabricated cell was evaluated and photovoltaic parameters were determined. The results showed the conversion efficiency of 0.17%, current density of ( $J_{sc}$ ) 0.69 mAcm<sup>-2</sup>, voltage ( $V_{oc}$ ) 0.38 v and fill factor (FF) of 0.69 under sun (Am1.5) for the cells. Electrochemical impedance spectroscopy (EIS) and cyclic voltammetry (CV) were employed to study the electron transfer mechanism in fabricated cells. The results showed that the potential in cathodic current was more positive indicating that the conduction band position of TiO<sub>2</sub> had shifted to positive energies confirming less  $V_{oc}$  of the fabricated cell.

**Keywords:** *Binuclear complex, Dye sensitized solar cells, Cyclic voltammetry, EIS.*

---

**\*Corresponding author:** *Mohammad Abedi, Department of Chemical Technologies, Iranian Research Organization for Science and Technology (IROST), Tehran, Iran. Email: mabedi50@yahoo.com, Tel: +982156276637.*

## Introduction

Dye sensitized solar cells (DSSCs) have been considered as one of the most promising alternative renewable energy sources since their first illustration by Michael Grätzel in 1991, attracting commercial and scientific attention due to their high conversion efficiency, low cost and simple manufacturing process [1-2]. Typically a DSSC is composed of transparent mesoporous film of semiconductor, which is often  $\text{TiO}_2$ , on a transparent conducting oxide (FTO) substrate that is covered with a monolayer of photosensitizer, an electrolyte consisting of redox couple (commonly  $\text{I}^-/\text{I}_3^-$ ) and platinized FTO as a counter electrode. By illumination of DSSCs, electrons are injected from LUMO of photoexcited dye to the conduction bands of the semiconductor. The sensitizer is regenerated by oxidizing  $\text{I}^-$  to  $\text{I}_3^-$  [3,4]. Although Ruthenium polypyridine complexes such as cis-bis (isothiocyanato) bis (2, 2'-bipyridyl-4, 4'-dicarboxylato) Ruthenium (II) bis-tetrabutylammonium (N719), cis-bis (isothiocyanato) bis (2, 2'-bipyridyl-4, 4'-dicarboxylato) Ruthenium (II) and tri (thiocyanato) (4, 4', 4''-tricarboxy 2, 2': 6', 2'' - terpyridine) Ruthenium (II) (black dye) are most commonly used sensitizers due to their broad absorption spectra and good photovoltaic performance, they are very expensive, therefore the replacement of them with cheaper photosensitizers has been suggested.

Sensitizers such as organic dyes (metal free), natural dyes extracted from plants and metal complexes such as porphyrins, Zinc and Copper and Zinc and Cobalt complexes with 0.5% to 4% efficiency have been used as photosensitizer in DSSCs [5-9]. So, synthesis and using novel and low cost dyes with high molar extinction coefficient are an attractive research option in the area of DSSCs. For non-Ruthenium sensitizers, dye aggregation on the surface of  $\text{TiO}_2$  is one of greatest challenges which diminishes the electron transfer and leads to decreased photovoltaic performance [10,11]. Since photosensitizers with non-planar structures prevents dye aggregation on the surface of the semiconductor and Copper and Zinc complexes form non-planar complexes with different organic ligands, specific attention has been focused on synthesis and application of these sensitizers in the performance of DSSCs [12-14]. In this work, a binuclear complex with unsymmetrical macrocyclic ligand containing two propionitrile pendant arms  $[\text{ZnLCu}(\text{OAC})]\text{PF}_6$  as a non-planar photosensitizer in dye sensitized solar cell as well as the photovoltaic performance of the cell have been evaluated.

## Experimental

### *Materials*

All chemicals were analytical grade and used as received without further purification.  $\text{TiCl}_4$ , Ethanol and  $\text{H}_2\text{PtCl}_6$  were purchased from Merck (Germany). N719 dye,  $\text{TiO}_2$  paste, Fluorine-doped  $\text{SnO}_2$  conductive glass (FTO) with  $15 \Omega \text{ cm}^{-2}$  resistances and Surlyn polymer film were obtained from Solaronix (Switzerland). The electrolyte solution (Iodolyte ELT-ACN-I Sharif Solar) was purchased from Sharif Solar Company (Iran).

### *Apparatus*

UV-Visible spectra were measured by Lambda 25 Perkin Elmer spectrophotometer. A potentiostat/galvanostat instrument (PGSTAT. 302N, Autolab, Eco-Chemie, The Netherlands) was utilized to perform cyclic voltammetry (CV) and electrochemical impedance spectroscopy (EIS) techniques. EIS data were analyzed and fitted by  $Z_{\text{view}}/Z_{\text{plot}}$  (Scribner Associate, Inc). The photocurrent-voltage (I-V) curves were measured utilizing the potentiostat/galvanostat equipment under simulated sunlight instrument SIM10 at  $100 \text{ mW cm}^{-2}$  and air mass 1.5 G illumination. Tescan Mira FE-SEM instrument was used to study the surface morphology of  $\text{TiO}_2$  layer on the FTO.

### *Preparation of Dyes*

The chemical structure of the dyes N719 and  $[\text{ZnLCu}(\text{OAC})]\text{PF}_6$  used for fabrication of DSSCs has been shown in Figure 1. The concentration of N719 dye solution was 0.3 mM in ethanol and 3.5 mM in acetonitrile for synthetic dye. The synthesis procedure for preparation of  $[\text{ZnLCu}(\text{OAC})]\text{PF}_6$  {L = 1, 6- bis (2-cyanoethyl) -2, 5-bis (2-hydroxy 3-formyl-5-methylbenzyl)-2, 5- diazahexane} has been mentioned before [15].

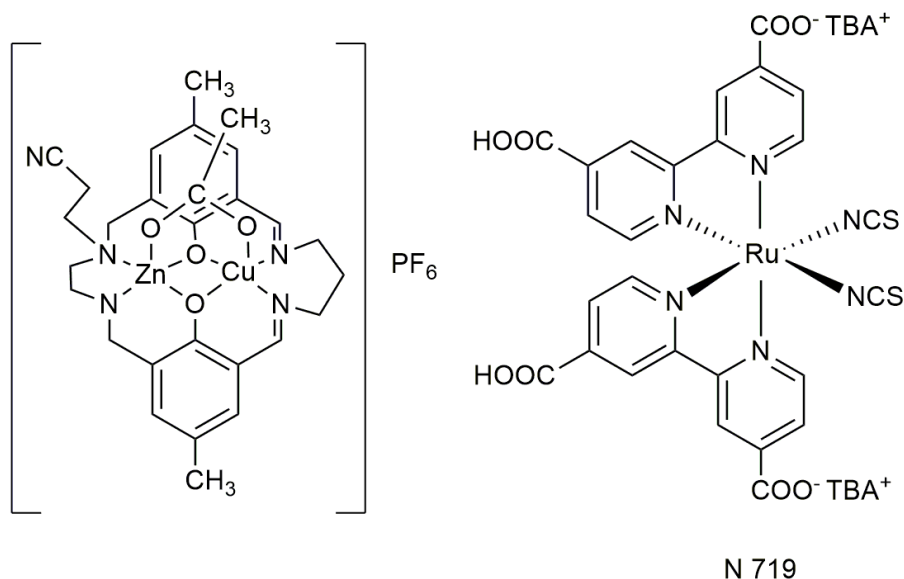


**Figure 1.** Chemical structure of [ZnLCu(OAC)PF<sub>6</sub>] and N719 dyes.

#### *Preparation of Photoanode*

The Fluorine doped tin oxide (FTO) glass with sheet resistance of  $15 \Omega \text{ cm}^{-2}$  glass was cut to the size of  $1.5 \times 1.5 \text{ cm}^2$  and cleaned under ultrasonic treatment (5 min in acetone, 5 min in alcohol), after washing with water to make both the working and counter electrodes. Pre-treatment of FTO was performed by immersing clean FTO in 40 mM aqueous TiCl<sub>4</sub> solution at 70 °C for 30 min (this treatment prevents recombination between FTO and electrolyte). Dr. Blade technique was utilized to deposit TiO<sub>2</sub> paste on FTO substrate (with the active of  $0.25 \text{ cm}^2$ ). The coated FTO was air-dried for about 5 min to reduce the surface irregularities, then sintered at 500 °C for 60 min to remove organic load. After cooling to the room temperature, Post-treatment was performed as pre-treatment conditions to prevent recombination between electrolyte and electrons in conduction band of TiO<sub>2</sub> followed by calcination at 500 °C for 60 min. After cooling to 80 °C, it was immersed in the dye solutions (N719 solution as reference and [ZnLCu(OAC)]PF<sub>6</sub> solution as new sensitizer) for 24 h to adsorb dyes. The photoelectrodes were rinsed with pure ethanol to remove any non-adsorbed dyes on the surface and dried at room temperature [16,17]. The morphology of the deposited TiO<sub>2</sub> was studied by scanning electron microscopy (SEM). Figure 2 shows the SEM image of photoelectrode obtained from Tescan Mira FE-SEM. The average size of TiO<sub>2</sub> nanoparticles was approximately 20 nm.

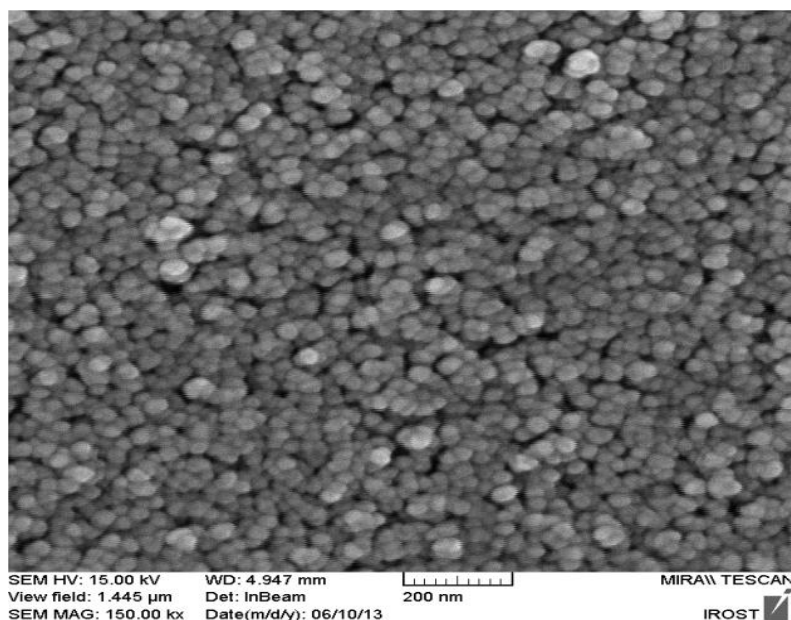


**Figure 2.** SEM image of TiO<sub>2</sub> nanostructure deposited on the surface of FTO.

#### *Preparation of Counter Electrode*

The cleaned FTO was drilled with 0.4 mm diameter drill bit and then two to three drops of H<sub>2</sub>PtCl<sub>6</sub> solution (0.5 M) were sprayed on the surface of FTO, followed by drying and heating at 460 °C for 15 min, resulting in the deposition of Pt on the surface by the drop casting technique [18].

#### *Fabrication of the Cells*

The dye-coated TiO<sub>2</sub> and Pt counter electrodes were assembled into a sandwich-type cell. The sealing of DSSC was done using a thermal adhesive film (Surlyn, Dyesol, 60-μm-thick) as spacer by keeping the structure in a hot-press at 120 °C for 90 sec. Finally a drop of electrolyte solution was injected into the cell via a hole which was predrilled at the back of the counter electrode by vacuum pump and then the filling hole was sealed with a small piece of glass [18].

## Results and discussion

### UV-Visible Absorption Spectra

UV-Visible absorption spectra of ZnCu complex dye before and after adsorption on the nanocrystalline TiO<sub>2</sub> are shown in Figure 3. The spectra of binuclear complexes included d-d transition and some metal-ligand charge transfer bands and formed the intense peak at 670 nm [15]. After adsorption on the surface of TiO<sub>2</sub>, this band shifted to a longer wavelength (677 nm). The red shift in the absorption peak after the immersion of TiO<sub>2</sub> in dye solution was attributed to the binding of the dye on the surface of porous TiO<sub>2</sub> [19,20].

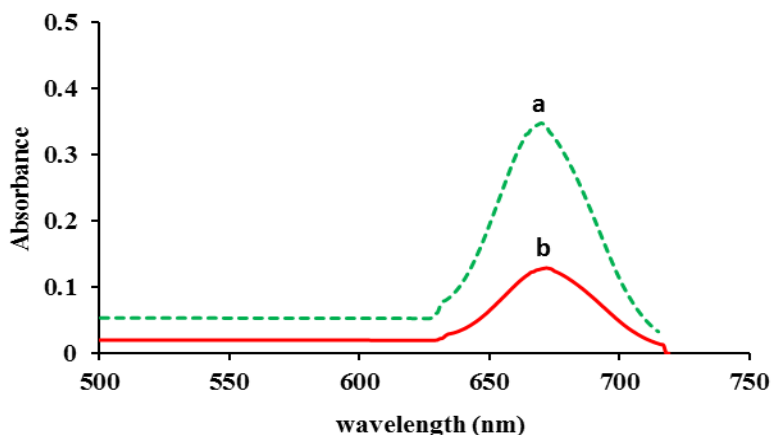


**Figure 3.** UV-Vis absorption spectra of Zn Cu complex dye in acetonitrile solution (a) and after adsorption on the surface of TiO<sub>2</sub> (b).

### J-V Characteristics and Performance of DSSCs

Current density-voltage (J-V) diagrams of fabricated cells were obtained using simulated solar light (Am 1.5, 100 mw cm<sup>-2</sup>). A standard silicone solar cell was used as a reference cell for calibrating the light intensity of the solar simulator. The lamp power of the solar simulator was adjusted to increase the short circuit current density ( $J_{sc}$ ) of the reference cell under simulated light as high as that of calibration conditions [21]. Figure 4 shows the J-V curves and photovoltaic parameters of cell using Zn Cu complex as sensitizer.

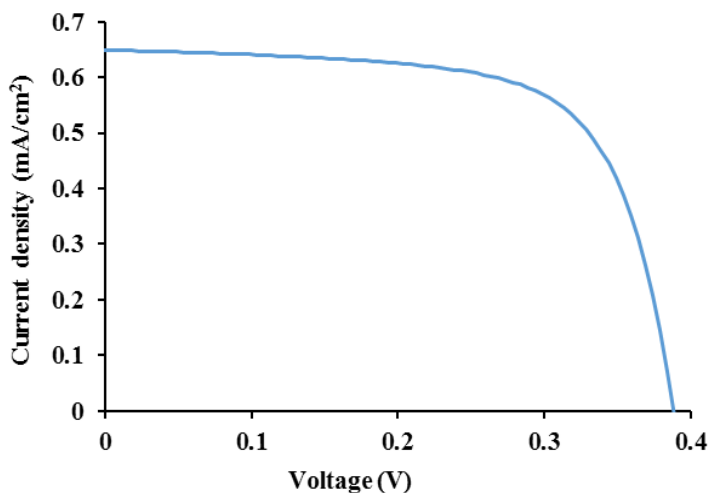


**Figure 4.** (J-V) curves of DSSC fabricated by Zn Cu Complex dye as sensitizer with photovoltaic parameters (Efficiency ( $\eta$ ) = 0.17%, Fill Factor (FF) = 0.69, Open circuit voltage ( $V_{oc}$ ) = 0.38 v, Short circuit current density ( $J_{sc}$ ) = 0.65 mA/cm<sup>2</sup>).

#### *Electrochemical Impedance Spectroscopic (EIS) Study*

Electrochemical Impedance Spectroscopy (EIS) is a powerful, non-destructive, and informative technique to study the electrical and electrochemical properties of the interfaces [22-24]. EIS was carried out at  $-V_{oc}$  bias in dark conditions with an electrochemical workstation at room temperature. The measured frequency range was from 100 KHz to 1 mHz, and the AC amplitude was set at 10 mV.

Figure 5 shows the typical Nyquist plot of our device. The semicircle profile of Nyquist plot of DSSC displays charge transfer resistances at different interfaces. However, the first semicircle corresponding to the high frequency region (100 kHz -100 Hz) indicates resistance at the electrolyte/Pt counter electrode interface ( $R_1 = R_{Pt}$ ). The second semicircle is associated with the intermediate frequency range (100 Hz-1 Hz) representing the charge transport resistance ( $R_t$ ) and charge transfer resistance ( $R_{ct}$ ) at the photoanode/dye/electrolyte interfaces. Also,  $R_s$  is attributed to the total resistance of the conducting glass sheet and solution [25]. The equivalent circuit used for fitting the impedance spectra of the DSSC is shown in Figure 6, the constant phase elements (CPEs) which include the two parameters  $CPE-T$  and  $CPE-P$ , demonstrate the non-ideal capacitance in the semicircles.

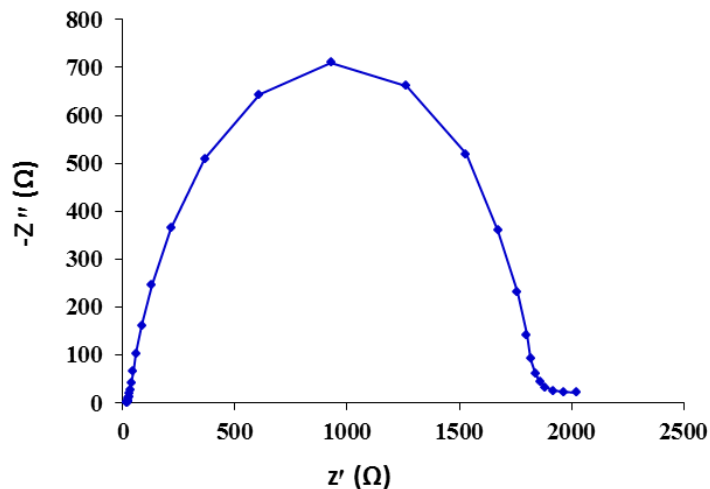


Figure 5. Nyquist plot of DSSC fabricated by Zn Cu Complex dye as sensitizer.

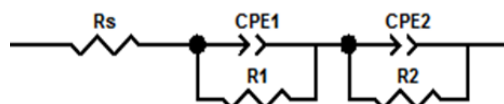


Figure 6. Equivalent circuit used for impedance data approximation.

All the values of the equivalent circuit parameters obtained from the EIS plot by fitting data with Zview/Zplot (Scribner Associates, Inc.) are reported in Table 1.

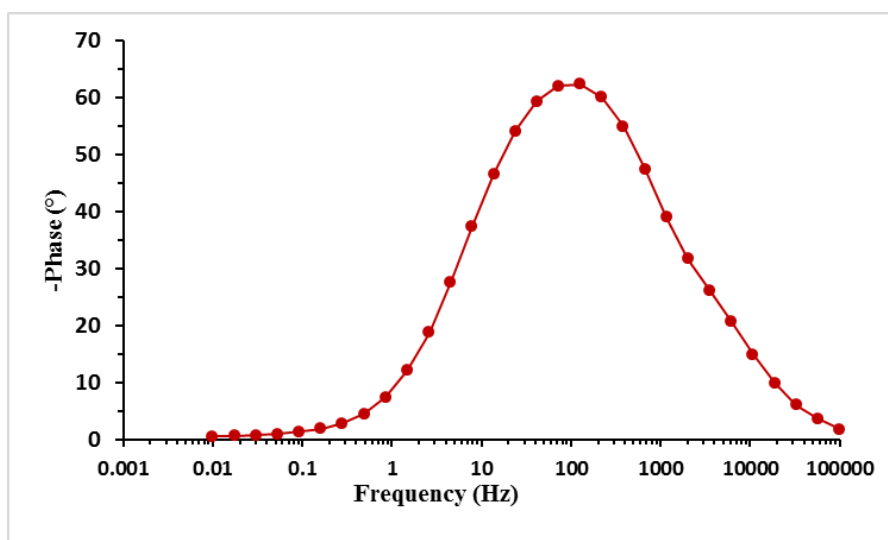


Figure 7. Bode plots of prepared DSSC based on Zn Cu Complex dye sensitizer.



The electron lifetime ( $\tau$ ) can be determined by either Bode or Nyquist plots.  $R_{ct}$  and chemical capacitance,  $C_{\mu}$ , can be gained from fitting the data of Nyquist plots to calculate the  $\tau$  via equations 1 to 3. Generally as in the Nyquist plot,  $\tau$  can be estimated by the medium frequency from Bode plot (Fig. 7) using equation 4. The  $f_{max}$  is the maximum frequency of semicircle arc at middle frequencies. The results show that the values from both methods are in satisfactory agreement with each other. Electron density in the conduction band of  $TiO_2$  ( $n_s$ ) can be obtained by equation 5 where  $L$ ,  $K_B$ ,  $T$ ,  $D$ ,  $q$ ,  $A$  represent film thickness, Boltzmann constant, absolute temperature, effective diffusion coefficient of electrons, respectively [25,26]. Electron lifetime in a  $TiO_2$  is associated with electron recombination reactions. In fact, the high amount of  $\tau$  indicates less recombination. Although  $\tau$  was higher in the case of using Zn Cu complex, electron density in the conduction band ( $n_s$ ) was lower, so the efficiency of fabricated cell decreased [10,27]. The low  $n_s$  value was associated with low absorption coefficient of Zn Cu complex in the visible range of illumination. Therefore, developing new efficient metal complex photosensitizers, an increase in the absorption coefficient of the metal complex in the visible region of sun light is needed.

$$\tau_{eff} = R_{ct} \times C_{\mu} \quad (1)$$

$$C_{\mu} = \frac{(R_{ct} \times CPE - T)^{1/CPE-P}}{R_{ct}} \quad (2)$$

$$\tau = (R_{ct} \times CPE - T)^{1/CPE-P} \quad (3)$$

$$\tau_{eff} = \frac{1}{\omega_{max}} = \frac{1}{2\pi f_{max}} \quad (4)$$

$$n_s = \frac{LTK_B}{ADq^2R_t} \quad (5)$$

**Table 1.** The comparison of electrochemical parameters of DSSCs fabricated by Zn Cu complex and N719 dye sensitizers.

No	Dye	$R_{ct}$ ( $\Omega$ )	$R_t$ ( $\Omega$ )	$D_{eff}$ ( $cm^2s^{-1}$ )	$\tau$ (ms)	$n_s$ ( $cm^{-3}$ )
1	ZnCu complex	1850	25	$1.36 \times 10^{-3}$	21.3	$7.81 \times 10^{17}$
2	N719 (Standard cell)	35	1.3	$9.36 \times 10^{-3}$	15.1	$1.07 \times 10^{19}$

### *Linear Sweep Voltammetry*

Cyclic voltammetry (CV) technique is an appropriate method to study the distribution and density of local state energy in DSSCs. Under forward bias, the cathodic current arises from the reduction of  $I_3^-$  species by electron injected from the FTO substrate into the mesoporous semiconductor  $TiO_2$ , while in reverse bias, anodic current is attributed to the regeneration process of dye molecule by oxidation of  $I^-$  ions in the electrolyte. The cathodic current can provide data about the position of the electronic Fermi level ( $E_F$ ). The forward bias is attributed to the difference between the electronic fermi level ( $E_F$ ) and redox potential of electrolyte ( $E_{redox}$ ). Therefore, according to the relationship between the current and forward bias, the onset potential in cathodic current indicates the position of the conduction band of  $TiO_2$  semiconductor (Figure 8A) [28]. The cyclic voltammetry measurements of fabricated cells were performed in dark light from -1.0 to 1.0 volt at scan rate of 50 mV/s.

As shown in Figure 8B, the onset potential in cathodic current for the  $TiO_2$  electrode sensitized with Zn Cu Complex has occurred at more positive potential in comparison to the electrode covered with N719, indicating that the conduction band position of  $TiO_2$  had shifted to positive energies confirming less  $V_{oc}$  for the fabricated cell using new synthetic dye and more electron transfer from the conduction band of  $TiO_2$  to  $I_3^-$  ions in the electrolyte. The type of dye also had a significant effect on the anodic current (oxidation of  $I^-$  to  $I_3^-$ ) under reverse bias (from less positive to more positive potentials). As shown in Figure 6B the onset potential in anodic current for the  $TiO_2$  electrode sensitized with Zn Cu complex has occurred at more positive potential in comparison with N719, indicating that the difference between HOMO state of dye and  $E_{redox}$  electrolyte increased in the case of Zn Cu complex. Thus, regeneration of dye by oxidation of  $I^-$  had been retarded with the lower anodic current representing the lower adsorption of dye on the surface of  $TiO_2$  nonporous electrode consequently [29]. The use of a new dye in DSSCs increased the anodic current under reverse bias and cathodic current under forward bias, showing that an appropriate sensitizer has been introduced.

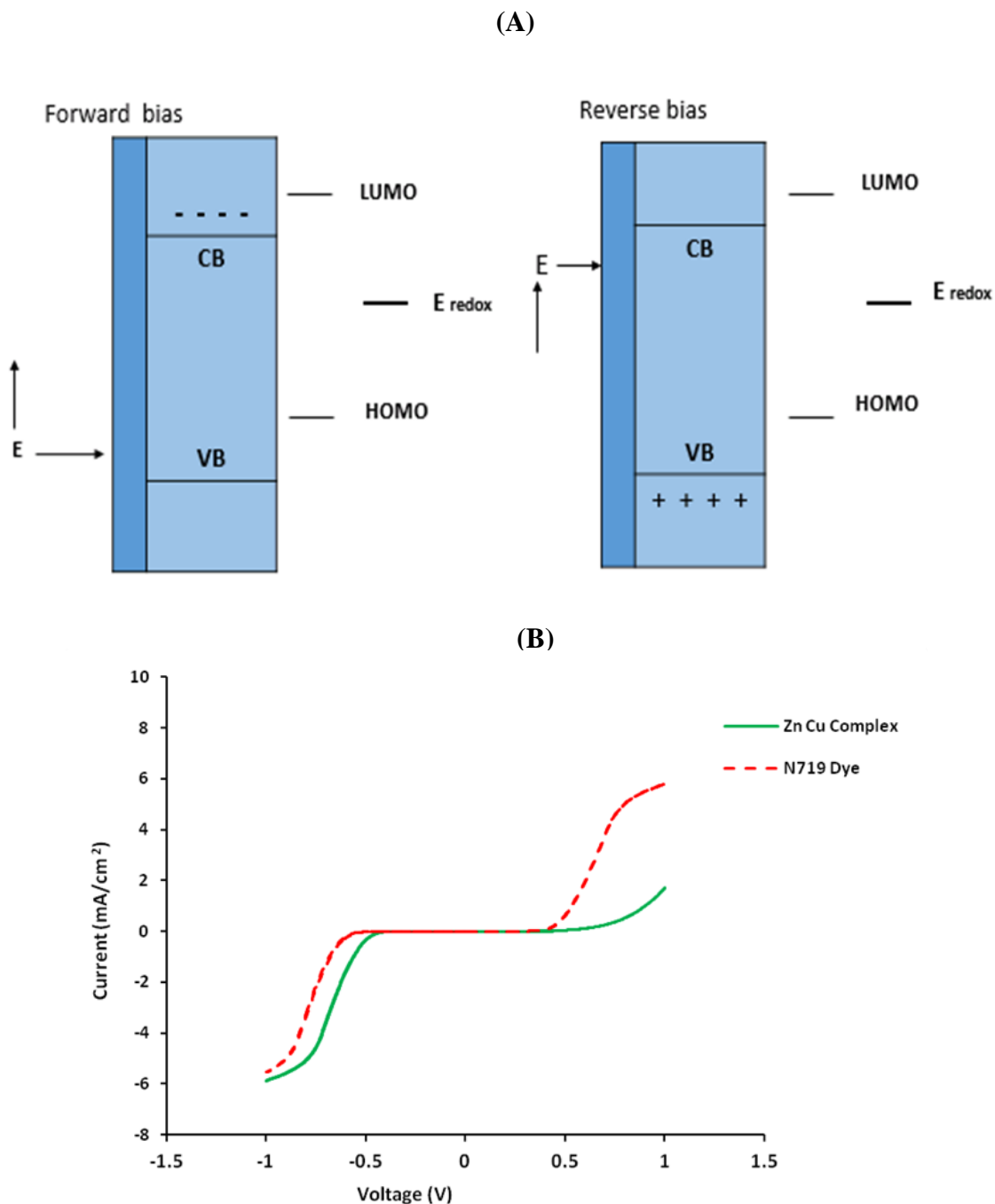


**Figure 8.** (A) a schematic diagram showing the interfacial charge-transfer processes at the dye-sensitized semiconductor electrode upon forward and reverse bias, (B) Cyclic voltammograms of the cells fabricated by Zn Cu complex as a new dye and N719 a as commercial dye. Measurements were performed in the dark and at room temperature with scan rate of 0.05 V/S from 1.0 to -1.0 V versus saturated calomel electrode (SCE) as reference and Pt wire served as counter electrodes.

*Incident photon to electron conversion efficiency (IPCE)*

For further characterization of fabricated cells, incident photon to current conversion efficiency (IPCE) tests was performed. IPCE has been defined in equation (6):

$$IPCE = LHE(\lambda) \times \phi_{inj} \times \eta_{col} \quad (6)$$

LHE ( $\lambda$ ) is light harvesting efficiency,  $\phi_{inj}$  is quantum yield in electron injection from excited dye molecules and  $\eta_{col}$  is the charge collecting efficiency of the charge transfer in the photoanode layer. LHE ( $\lambda$ ) is the ratio of charge carrier numbers to the incident photons with wavelength ( $\lambda$ ) and is associated with amount of dye adsorbed on the surface of TiO<sub>2</sub>, thickness of TiO<sub>2</sub> and extinction coefficient of dye.  $\phi_{inj}$  is related to difference between energy level of excited dye and conduction band of TiO<sub>2</sub>. More difference causes stronger driving force and faster charges transfer. Based on equation (7),  $\eta_{col}$  also depends on  $K_t$  and  $K_r$ , where,  $K_t$  is transport rate constant and  $k_r$  is recombination rate constant [30,31].

$$\eta_{col} = \frac{k_t}{k_t + k_r} \quad (7)$$

Figure 9 shows IPCE spectra of DSSC sensitized by this new synthetic dye. The shape of IPCE spectra was very similar to UV-Vis absorption spectra of dye. Maximum peak at 400 nm is associated with the absorption of TiO<sub>2</sub> itself and maximum peak at 640 nm is related to injection of electrons from dye excited state to the conduction band of TiO<sub>2</sub> [32]. The low IPCE for [ZnLCu(OAC)]PF<sub>6</sub> was assigned to the poor attachment of dye to the surface of TiO<sub>2</sub>.

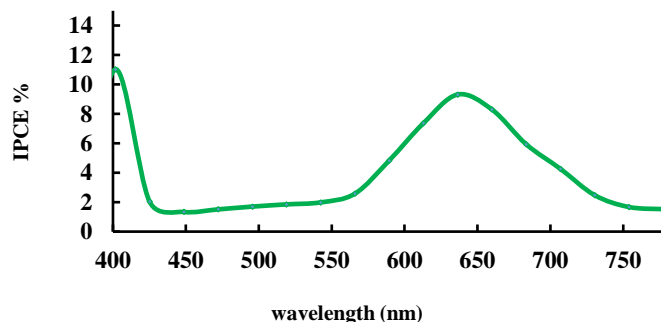


**Figure 9.** The IPCE curves of DSSC based on [ZnLCu(OAC)]PF<sub>6</sub> sensitizer.

## Conclusion

This study reported successful fabrication of DSSC sensitized with binuclear complex of [ZnLCu(OAC)]PF<sub>6</sub> {L = 1, 6- bis (2-cyanoethyl) -2, 5-bis (2-hydroxy 3-formyl-5-methylbenzyl)-2, 5- diazahexane}. The photovoltaic data of the cell were obtained and the EIS technique was utilized to study the electrochemical parameters and the results were compared with a standard cell based on N719 Ruthenium dye. The efficiency of fabricated DSSCs cell was low (0.17 %) but we hope that further molecular design of binuclear complexes opens up a new approach for synthesis and application of similar complexes in dye sensitized solar cells with higher efficiency.

## Acknowledgment

We acknowledge Iranian Research Organization for Science and Technology (IROST) for financially supporting this study. We thank Dr. Ramin Rahmani for improving the language of the manuscript.

## References

- [1] B. O Regan, M. Gratzel, *Nature.*, 353, 737 (1991).
- [2] D.W. Chang, H.N. Tsao, P. Salvatori, F.D. Angiles, M. Gratzal, S.M.Park, L. Die, H.J. Lee, J.B. Baek, M.K. Nazeeruddin, *RSC Adv.*, 2, 6209 (2012).
- [3] M. Gratzel, *J. Photochem. Photobiol. A. Chem.*, 164, 3 (2004).
- [4] M.K. Nazeeruddin, R.H. Baker, P. Liska, M. Grätzel, *J. Phys. Chem. B.*, 107, 8981 (2003).
- [5] J.N. Clifford, E.M.N. Ferrero, A. Viterisi, E. Palomares, *Chem. Soc. Rev.*, 40, 1635 (2011).
- [6] L.N. Ashbrook, C.M. Elliott, *J. Phys. Chem. C.*, 117, 3853 (2013).
- [7] T.E. Hewat, L.J. Yellowlees, N. Robertson, *Dalton Trans.*, 43, 4127 (2014).
- [8] A.O. Biroli, F. Tessore, M. Pizzotti, C. Biaggi, R. Ugo, S. Caramori, A. Aliprandi, C.A. Bignozzi, F.D. Angelis, G. Giorgi, E. Licandro, E. Longhi, *J. Phys. Chem. C.*, 115, 23170 (2011).
- [9] M. Khalili, M. Abedi, H. Sala Amoli, *Ionics*, 23, 779 (2017).
- [10] M. Afrooz, H. Dehghani, *RSC Adv.*, 5, 50483 (2015).
- [11] O. Bagheri, H. Dehghani, M. Afrooz, *RSC Adv.*, 5, 86191 (2015).

- [12] X. Lu, S. Wei, C.M.L. Wu, S. Li, W. Guo, *J. Phys. Chem. C.*, 115, 3753 (2011).
- [13] J.B. Lopez, N.F. Holguin, J.C.Gonzalez, D.G. Mitnika, *J. Photochem. Photobiol. A.*, 267, 1 (2013).
- [14] S. Hattori, Y. Wada, S. Yanagida, S. Fukuzumi, *J. AM. CHEM. SOC.*, 127, 9648 (2005).
- [15] H. Golchoubian, D. Sadeghi Fateh, G. Bruno, H. A. Rudbari, *J. Coord. Chem.*, 65, 1970 (2012).
- [16] M. Afrooz, H. Dehghani, *J. Power Sources.*, 262, 140 (2014).
- [17] A. Sedghi, H.N. Miankushki, *Jpn. J. Appl. Phys.*, 52, 75002 (2013).
- [18] S.A. Mozaffari, M. Ranjbar, E. Kouhestanian, H. Salar Amoli, M. H. Armanmehr, *Mater. Sci. Semicond. Process.*, 40, 285 (2015).
- [19] K.V. Hemalatha, S.N. Karthick, C. Justin Raj, N-K Hong, S-K Kim, H-J Kim, *Spectrochim. Acta, A.*, 96, 305 (2012).
- [20] G. Calogero, G. D. Marco, *Sol. Energy Mater. Sol. Cells.*, 92, 1341 (2008).
- [21] K. A. Emery, C. R. Osterwald, *Solar Cells.*, 17, 253 (1986).
- [22] F.F. Santiago, J. Bisquert, G.G. Belmonte, G. Boschloo, A. Hagfeldt, *Sol. Energy Mater. Sol. Cells.*, 87, 117 (2005).
- [23] Q. Wang, J. E. Moser, M. Gratzel, *J. Phys. Chem. B.*, 109, 14945 (2005).
- [24] M. Adachi, M. Sakamoto, J. Jiu, Y. Ogata, S. Isoda, *J. Phys. Chem. B.*, 110, 13872 (2006).
- [25] M. Samadpour, N. Taghavinia, A. Irajizad, M. Marandi, F. Tajabadi, *Eur. Phys. J. Appl. Phys.*, 57, 20401 (2012).
- [26] M. Ranjbar, S.A Mozaffari, E. Kouhestanian, H. Salar Amoli, *J. Photochem. Photobiol. A.*, 321, 110 (2016).
- [27] M. Afrooz, H. Dehghani, *Org. Electron.*, 29, 57 (2016).
- [28] Q. Wang, Z. Zhang, S. M. Zakeeruddin, M. Gratzel, *J. Phys. Chem. C.*, 112, 7084 (2008).
- [29] B. Li, J. Chen, J. Zheng, J. Zhao, Z. Zhu, H. Jing, *Electrochim. Acta.*, 59, 207 (2012).
- [30] G. Calogero, J-Ho Yum, A. Sinopoli, G. Di Marco, M. Gratzel, M.K. Nazeeruddin, *Solar energy.*, 86, 1563 (2012).
- [31] P. Dua, L. Song, J. Xiong, N. Li, Z. Xi, L. Wang, D. Jin, S. Guo, Y. Yuan, *Electrochim. Acta.*, 78, 392 (2012).
- [32] P. Luo, H. Niu, G. Zheng, X. Bai, M. Zhang, W. Wang, *Spectrochim. Acta, Part A.*, 74, 936 (2009).